

Farhad Bahmanpouri¹, Silvia Barbeta¹, Xinqi Hu², Zhen Zhou³, Daniel Wennerberg⁴, Angelica Tarpanelli¹, Peter Bauer-Gottwein⁵

¹ Research Institute for Geo-Hydrological Protection, National Research Council (CNR-IRPI), Via Madonna Alta 126, 06128 Perugia, Italy. Email: farhadbahmanpouri@cnr.it
² Chair of Hydrology and River Basin Management, Technical University of Munich, Germany
³ DTU Space, Technical University of Denmark, Kgs. Lyngby, Denmark
⁴ Swedish Meteorological and Hydrological Institute, 601 76 Norrköping, Sweden
⁵ Department of Geosciences and Natural Resource Management, University of Copenhagen, Øster Voldgade 10, 1350 Copenhagen

Abstract

This study emphasizes the significance of river monitoring for flood risk reduction and water resource management. The Entropy model was employed to estimate velocity distribution and discharge based on surface velocity and bathymetry data in three cross-sections along the Rönne River in Sweden.

Key Points:

- Three river cross-sections over 10 km of the Rönne River were surveyed.
- Surface velocities measured using:
 - OTT MF Pro (electromagnetic sensor)
 - UAS RGB camera videos analyzed via PIV and STIV methods.
- Bathymetry data collected using water-penetrating radar.
- The Entropy model estimated 2D velocity distribution and river discharge.
- Velocity dip phenomena (maximum velocity below the surface) was accounted for in low aspect ratio sections.
- Discharge was calculated using mean velocity and flow area.
- The integrated approach (UAS data + Entropy model) proved accurate and safe for monitoring, especially in inaccessible or high-flow conditions.

Research methodology

The velocity distribution is based on surface velocity according Chiu (1989) and consequently Moramarco et al. (2004):

$$U(x_i, y) = \frac{U_{max}(x_i)}{M} \ln \left[1 + (e^M - 1) \frac{y}{D(x_i) - h(x_i)} \exp \left(1 - \frac{y}{D(x_i) - h(x_i)} \right) \right] \quad i = 1 \dots N_v \quad (1)$$

For gauged sites:

$$\phi(M) = U_m / U_{max} = \left(\frac{e^M}{e^M - 1} - \frac{1}{M} \right)$$

For ungauged sites (Moramarco and Singh, 2010):

$$\phi(M) = \frac{1}{k} \left[\ln \left(\frac{y_{max}}{y_o} \right) + \frac{h}{y_{max}} \ln \left(\frac{h}{D} \right) \right]$$

Velocity dip (Yang et al. 2004):

$$\delta(x_i) = 1 + 1.3e^{-x_i/D(x_i)}$$

$$\delta(x_i) = \frac{D(x_i)}{D(x_i) - h(x_i)}$$

$$U_{max}(x_i) = \frac{U_{surf}(x_i \cdot D(x_i))}{\frac{1}{M} \ln [1 + (e^M - 1) \delta(x_i) e^{1 - \delta(x_i)}]}$$

U_m : Depth averaged velocity,
 U_{max} : Maximum velocity,
 y_{max} : the location of u_{max} ,
 k : the von Karman constant,
 $D(x_i)$ is the flow depth,
 $h(x_i)$ is the dip-location

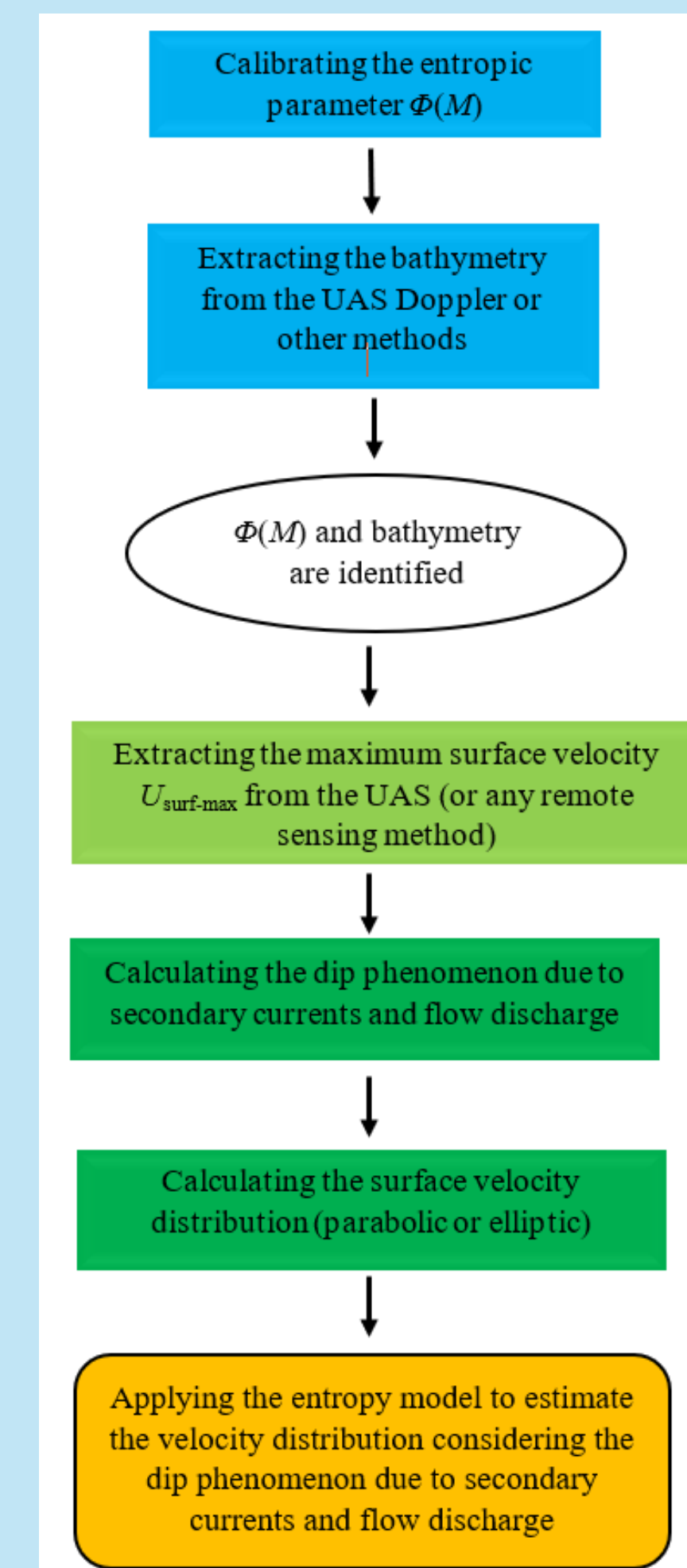


Figure 1: workflow for the estimation of the flow velocity and river discharge

Study area

The Rönne Å survey is part of the EU Horizon project UAWOS. The Rönne Å survey in Southern Sweden survey was carried out in August/September 2023.

The dataset contains water surface elevation, bathymetry, land elevation and water surface velocity datasets collected using different drone-borne and in-situ sensors (Figure 2).

Selected cross-sections measured by the UAS-borne RSS-2-300W Doppler radar were shown in solid circles (Figure 3).



Figure 2: Measured locations in Rönne River in Sweden

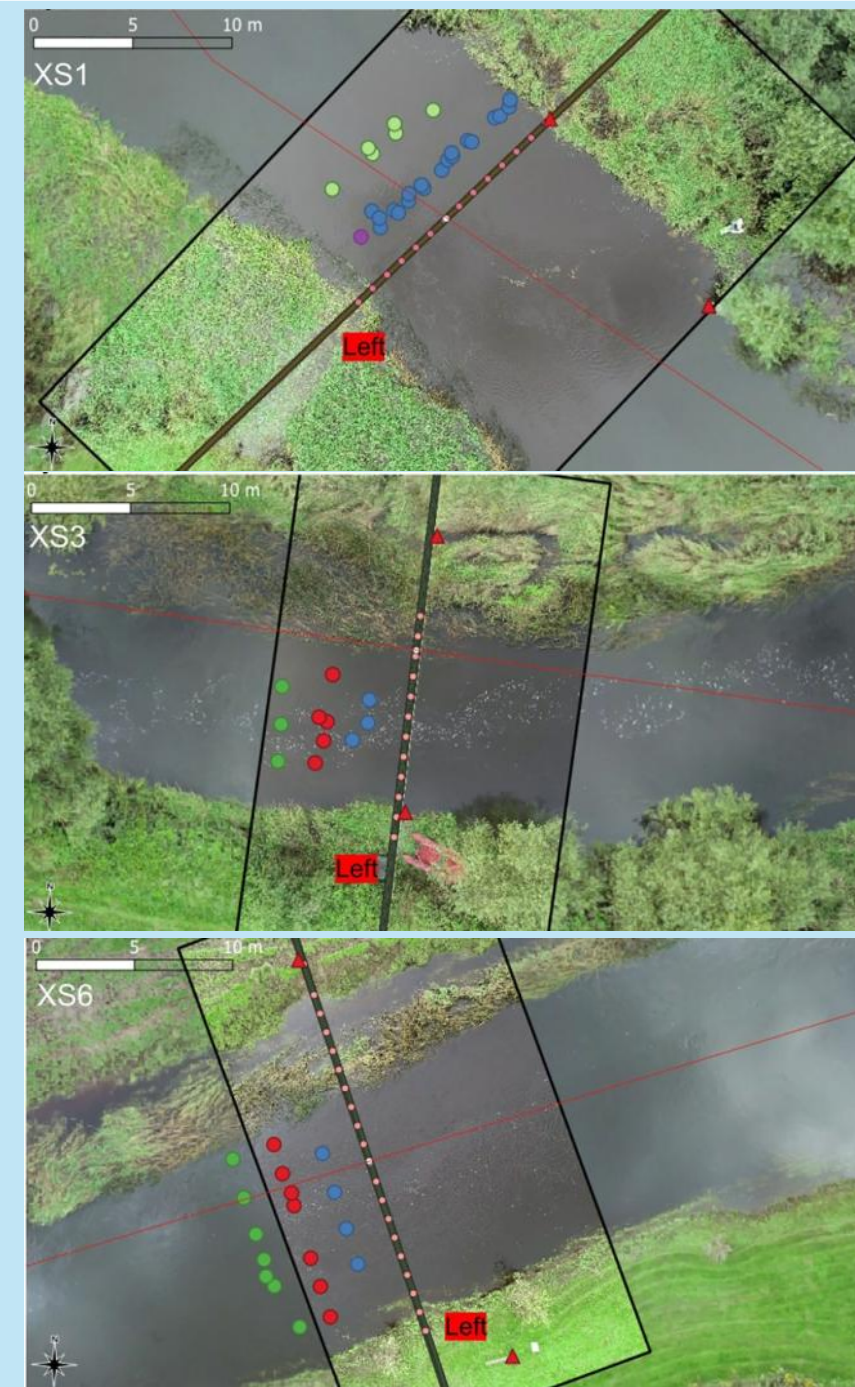


Figure 3: Selected cross-sections (N.1= XS1, N.3=XS3, N.6=XS6), Zhou et al. (2024)

Results

1. Calibrating the entropic parameter M

The magnitude and range of the entropic parameter M are consistent with findings from earlier studies, such as Bahmanpouri et al. (2022a) for large rivers, and Chiu et al. (2000), Bahmanpouri et al. (2022b) for smaller rivers. The entropic parameter M serves as an essential indicator reflecting the characteristics of a river cross-section, including variations in bed morphology, channel slope, and geometry (Chin and Murray, 1992). The physical meaning of the function $\phi(M)$ is in its ability to represent channel and flow properties through the relationship between mean and maximum flow velocities (Moramarco and Singh, 2010).

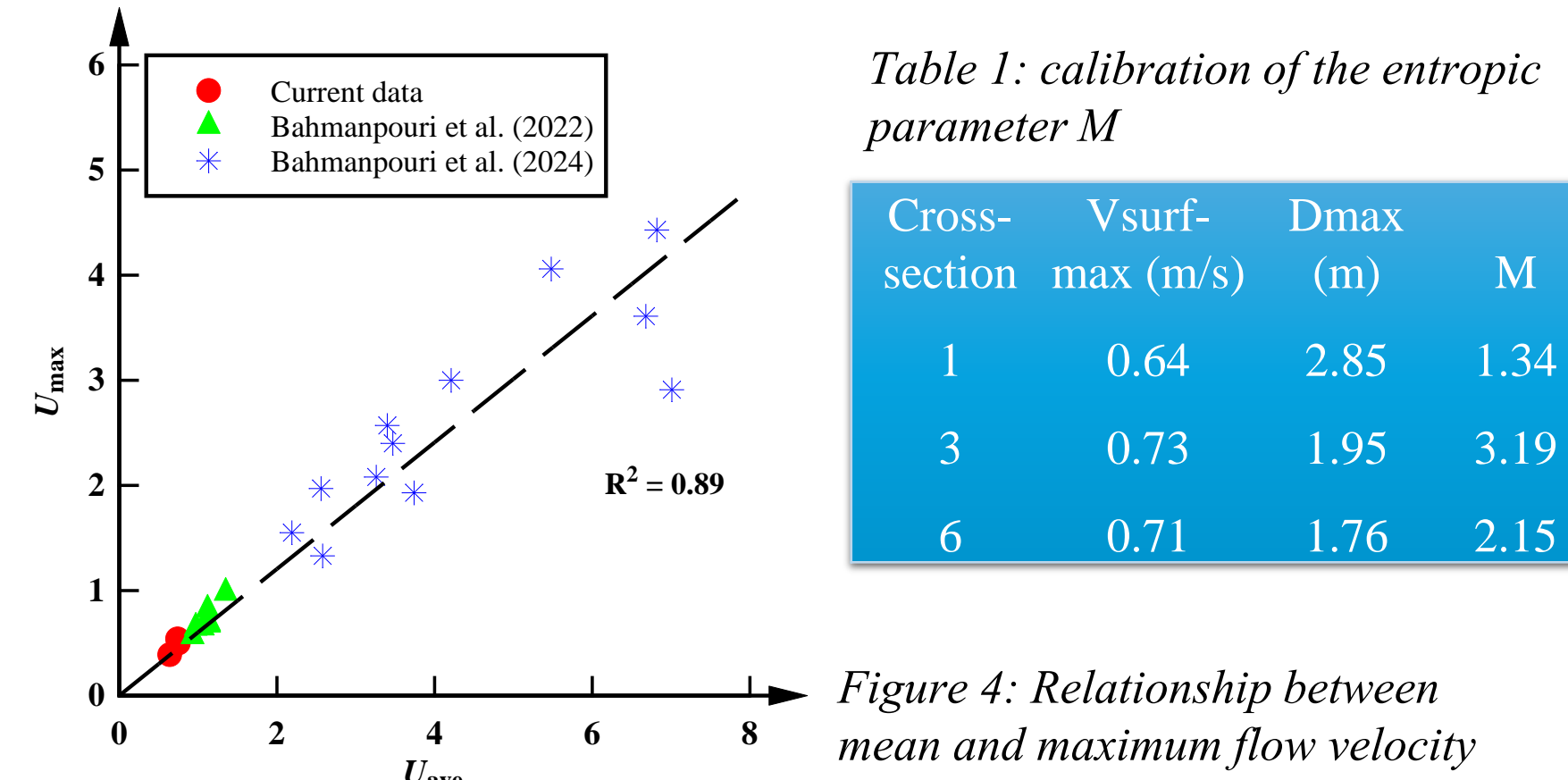


Figure 4: Relationship between mean and maximum flow velocity

2. Entropy, first scenario: all surface velocity

Figure 5 shows the cross-sectional distribution of the velocity using the Entropy model by considering all the surface velocities as input for the model.

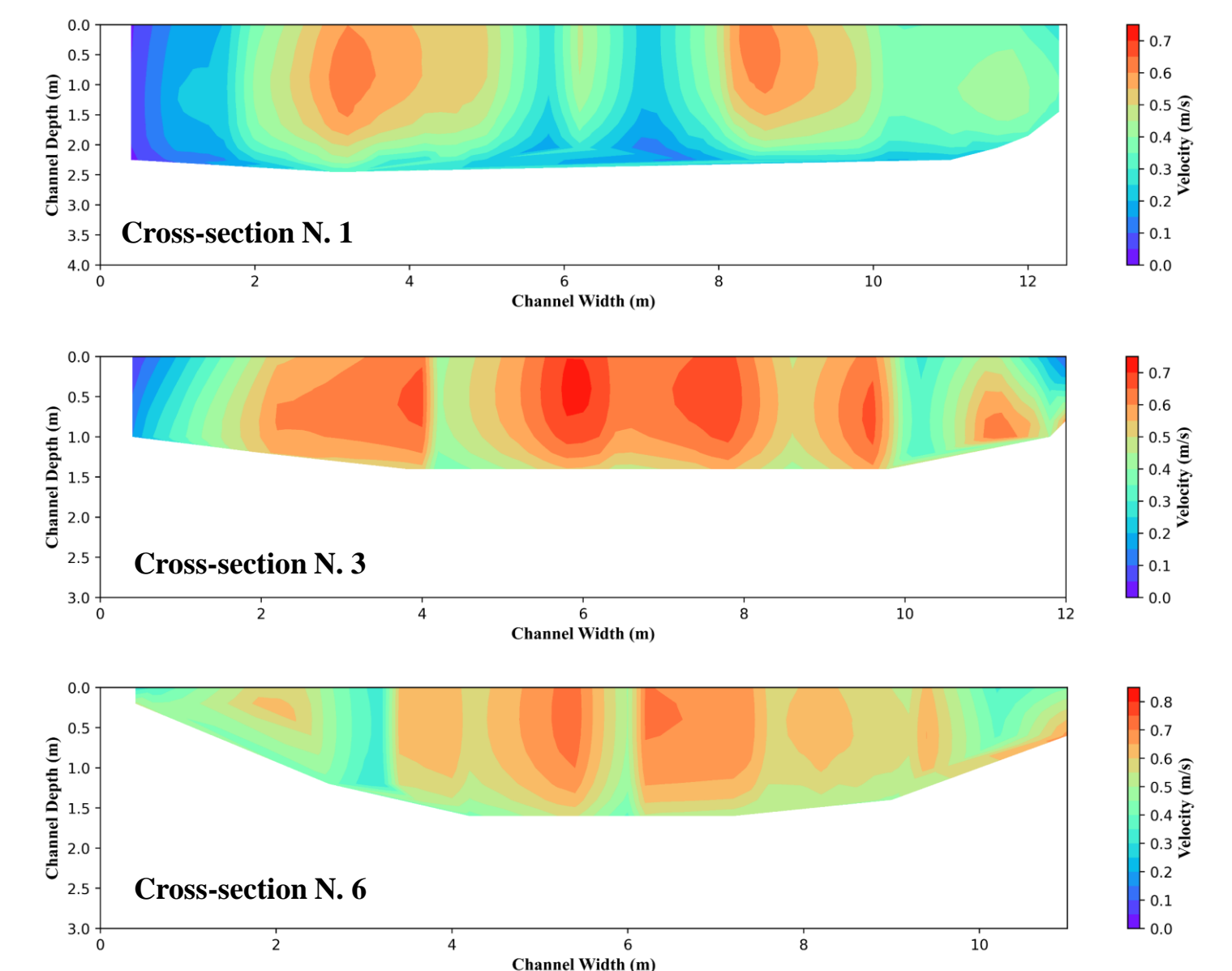


Figure 5: Cross-sectional velocity distributions

Table 2: Estimated discharge based on Entropy model for different cross-sections

Cross-section	Mean velocity (m/s)	Discharge (m ³ /s)
1	0.38	11.5
3	0.52	8.9
6	0.57	7.8

3. Entropy, second scenario: a single surface velocity

For each cross-section, first, the observed surface velocity distribution (Figure 6-8) as well as mathematical parabolic and elliptic distribution of the surface velocity (Figure 9-11) in the Entropy model is presented. Following that, the cross-sectional distribution of the velocity using the Entropy model by considering only maximum surface velocity as input for the model is shown.

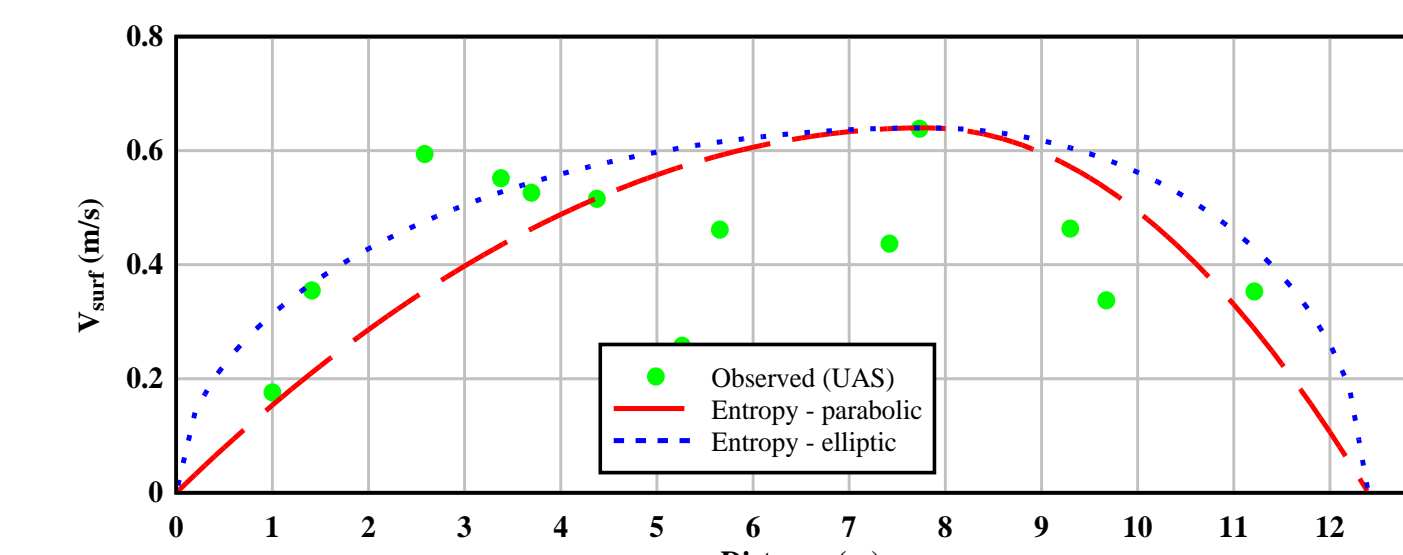


Figure 6: Surface velocity distribution for cross-section N.1

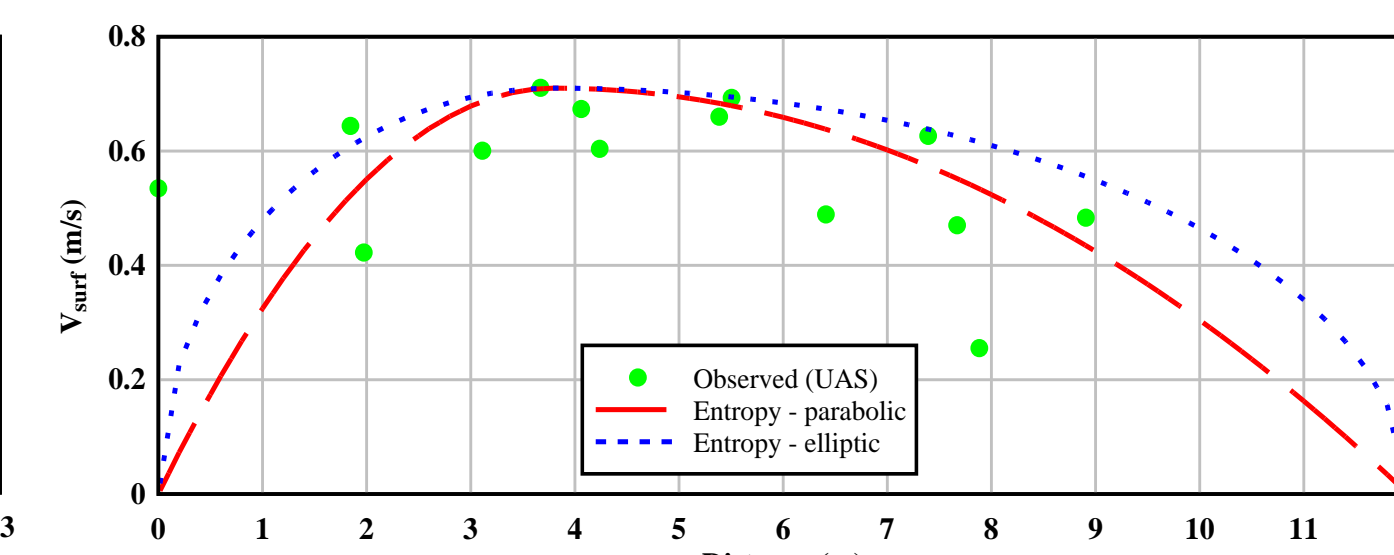


Figure 7: Surface velocity distribution for cross-section N.3

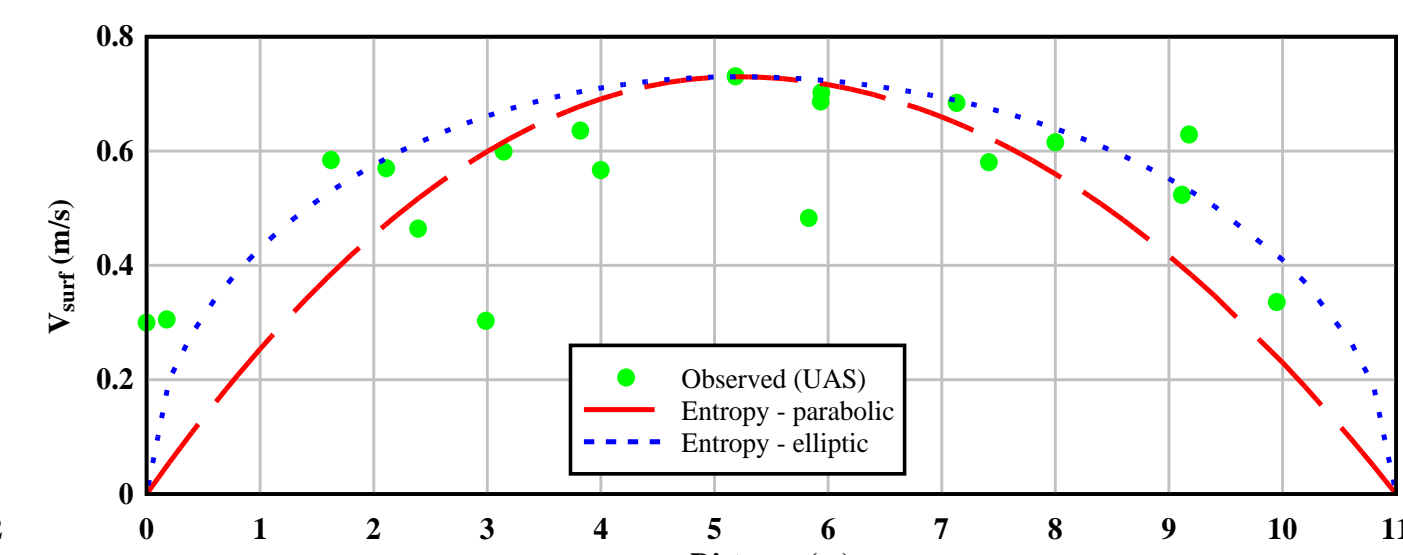


Figure 8: Surface velocity distribution for cross-section N.6

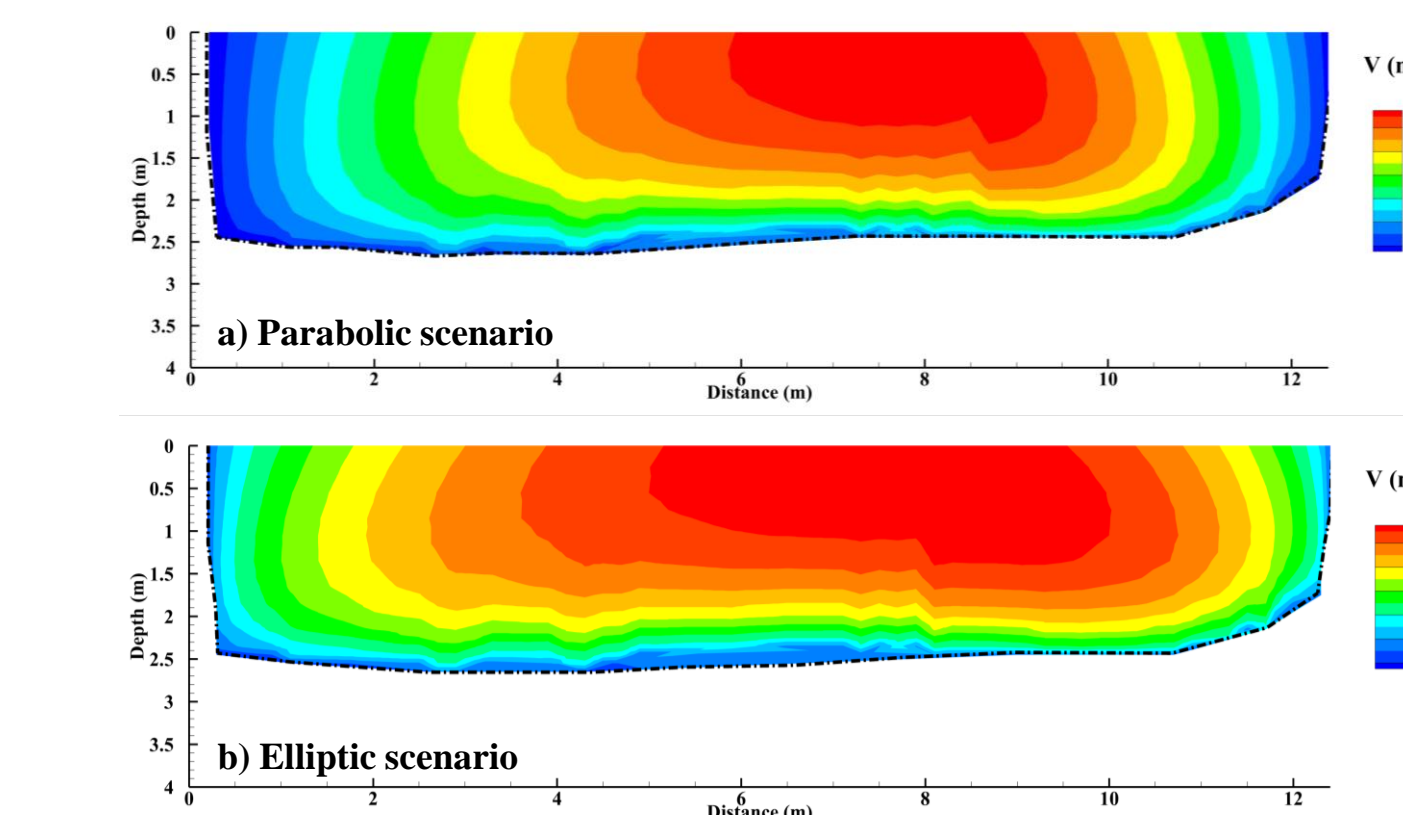


Figure 9: Velocity distribution for cross-section N.1

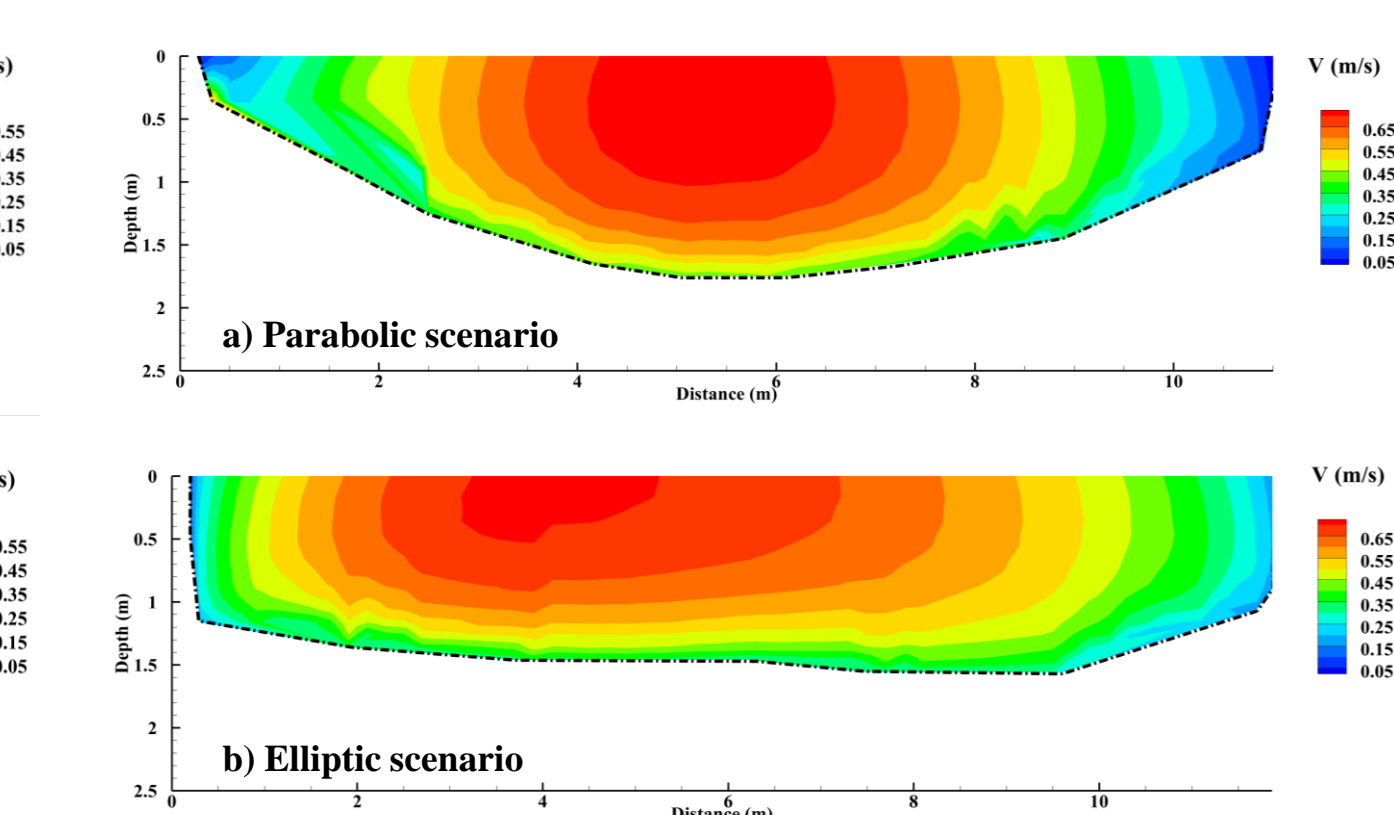


Figure 10: Velocity distribution for cross-section N.3

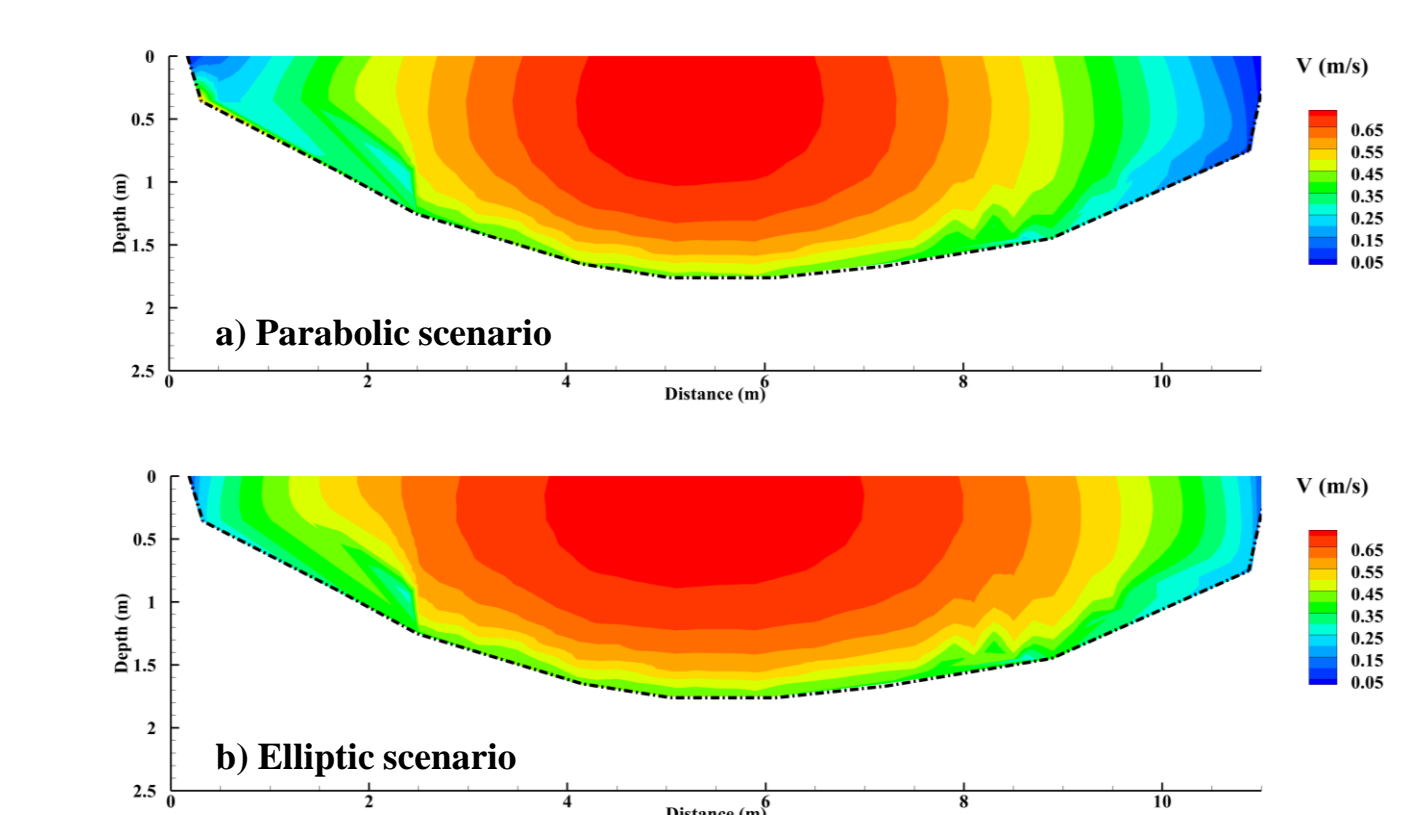


Figure 11: Velocity distribution for cross-section N.6

Table 3: Estimated discharge based on Entropy model considering two different scenarios of parabolic and elliptic surface velocity distribution

Cross-section	Mean velocity (m/s)		Discharge (m ³ /s)	
	Parabolic	Elliptic	Parabolic	Elliptic
1	0.39	0.47	12.3	14.9
3	0.54	0.59	8.1	8.8
6	0.50	0.53	9.1	9.7

4. Velocity dip

For the channels with an aspect ratio (river width/depth) less than 5 that is considered as a narrow channel, there is a possibility of velocity dip formation (see Table 4). Velocity dip is induced by the existence of the secondary currents in flow.

Table 4: Characteristics of the analyzed cross-sections

Cross-section	River width	Flow depth	Aspect ratio
1	12.4	2.85	4.4
3	12	1.76	6.8
6	11	1.95	5.6

Secondary currents results in:

- Vertical shift in momentum
- Enhance the turbulence and shear stress near the bed
- Increase the sediment transport rate

Results for the second scenario show that a velocity dip forms in all cross-sections (Figure 12). Notably, cross-section 1 exhibits a more pronounced velocity dip. This can be attributed to its lower aspect ratio (4.4), which is below the critical threshold of 5.

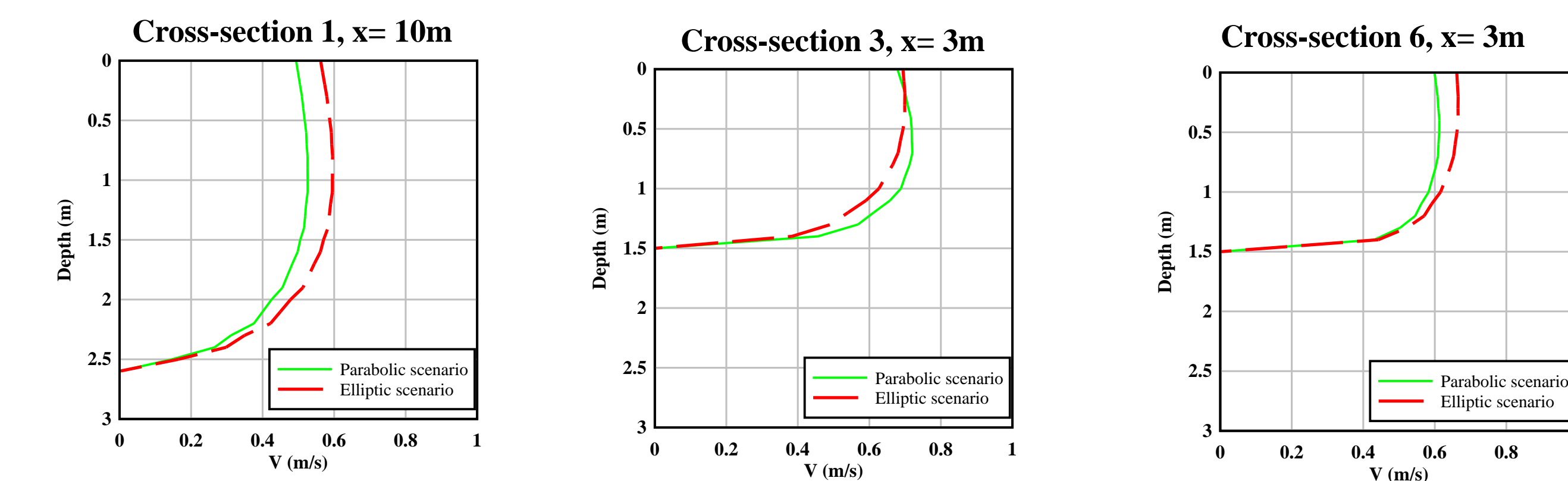


Figure 12: Vertical distribution of the velocity at different distance x for all the investigated cross-sections.

Conclusion

The results confirm that the proposed methodology can provide high-resolution, non-contact measurements, making it especially valuable for flow monitoring in remote or hazardous riverine environments during high-flow conditions.

Key benefits of this integrated approach include:

- **Improved safety** by minimizing the need for in-situ measurements during extreme events.
- **Enhanced spatial and temporal coverage** through UAS-based observations.
- **Cost-effective monitoring** with reduced manpower and equipment requirements.
- **Scalability and adaptability** to different riverine environments and hydrological conditions.

The outcomes of this research, pave the way for advanced, non-invasive river monitoring strategies that can significantly support water resource management and hazard mitigation efforts globally.

Further developments will be addressed to apply the Entropy model to other stations/ivers within the project and to derive rating curve and hence river discharge.

References

- Bahmanpouri, F., Barbeta, S., Gualtieri, C., Ianniruberto, M., Filizola, N., Termini, D., & Moramarco, T. (2022). Prediction of river discharges at confluences based on Entropy theory and surface-velocity measurements. *Journal of Hydrology*, 606, 127404.
- Bahmanpouri, F., Eltner, A., Barbeta, S., Bertalan, L., & Moramarco, T. (2022). Estimating the average river cross-section velocity by observing only one surface velocity value and calibrating the entropic parameter. *Water Resources Research*, 58(10), e2021WR031821.
- Chin, C. L., & Murray, D. W. (1992). Variation of velocity distribution along nonuniform open-channel flow. *Journal of Hydraulic Engineering*, 118(7), 989-1001.
- Chiu, C. L., Jin, W., & Chen, Y. C. (2000). Mathematical models of distribution of sediment concentration. *Journal of Hydraulic Engineering*, 126(1), 16-23.
- Moramarco, T., & Singh, V. P. (2010). Formulation of the entropy parameter based on hydraulic and geometric characteristics of river cross sections. *Journal of Hydrologic Engineering*, 15(10), 852-858.
- Zhou, Z., Riis-Klinkvort, L., Jørgensen, E. A., Lindenhoff, C., Frías, M. C., Vesterhauge, A. R., ... & Bauer-Gottwein, P. (2024). Measuring river surface velocity using UAS-borne Doppler radar. *Water Resources Research*, 60(11), e2024WR037375.

Aknowledgement

This research is funded by the EU's Horizon Europe under the UAWOS project (<https://uawos.dtu.dk/>)